Entanglement with negative Wigner function of three thousand atoms heralded by one photon

Entanglement with negative Wigner function of three thousand atoms heralded by one photon

Journal of Physics: Conference Series **723** (2016) 012054 doi:10.1088/1742-6596/723/1/012054

Entanglement with negative Wigner function of three thousand atoms heralded by one photon

Robert McConnell[1], Hao Zhang[1], Jiazhong Hu[1], Senka Ćuk[1,2] and Vladan Vuletić[1]

[1] Department of Physics, MIT-Harvard Center for Ultracold Atoms, and Research Laboratory of Electronics, Massachusetts Institute of Technology, Cambridge, Massachusetts 02139, USA
[2] Institute of Physics, University of Belgrade, Pregrevica 118, 11080 Belgrade, Serbia

E-mail: vuletic@mit.edu

Abstract. Quantum-mechanically correlated (entangled) states of many particles are of interest in quantum information, quantum computing and quantum metrology. Metrologically useful entangled states of large atomic ensembles have been experimentally realized [1, 2, 3, 4, 5, 6, 7, 8, 9, 10], but these states display Gaussian spin distribution functions with a non-negative Wigner function. Non-Gaussian entangled states have been produced in small ensembles of ions [11, 12], and very recently in large atomic ensembles [13, 14, 15]. Here, we generate entanglement in a large atomic ensemble via the interaction with a very weak laser pulse; remarkably, the detection of a single photon prepares several thousand atoms in an entangled state. We reconstruct a negative-valued Wigner function, an important hallmark of nonclassicality, and verify an entanglement depth (minimum number of mutually entangled atoms) of 2910 ± 190 out of 3100 atoms. Attaining such a negative Wigner function and the mutual entanglement of virtually all atoms is unprecedented for an ensemble containing more than a few particles. While the achieved purity of the state is slightly below the threshold for entanglement-induced metrological gain, further technical improvement should allow the generation of states that surpass this threshold, and of more complex Schrödinger cat states for quantum metrology and information processing.

1. Introduction

Many state-of-the-art atomic microwave clocks and interferometers based on atomic ensembles are limited no longer by technical noise, but rather by the fundamental quantum fluctuations of uncorrelated atoms, known as the standard quantum limit (SQL). Entangled states can improve measurement sensitivity beyond this limit using controlled correlations between atoms and represent important resources in quantum metrology. To date, metrologically useful spin-squeezed states [1, 2, 3, 4, 5, 6, 7, 8, 9, 10] have been produced in large ensembles. However, those moderately spin-squeezed states have Gaussian spin distributions and therefore can be viewed as semi-classical. Entanglement enters only to set a reduced amount of spin noise compared to the SQL. Non-Gaussian spin states with a negative Wigner function are however manifestly non-classical, since the Wigner function as a quasiprobability function must remain non-negative in the classical realm. They can be used for realizing quantum sensors which surpass the SQL since the non-Gaussian spin distributions can possess large Fisher information.

Here we generate entanglement in a large atomic ensemble by detecting a single photon that has interacted with the ensemble [16]. An incident vertically polarized photon experiences a

weak random polarization rotation associated with the quantum noise of the collective atomic spin. The detection of a horizontally polarized emerging photon then heralds a non-Gaussian entangled state of collective atomic spin (Figure 1) with a negative-valued Wigner function of -0.36 ± 0.08, and an entanglement depth of 90% of our ensemble containing several thousand atoms.

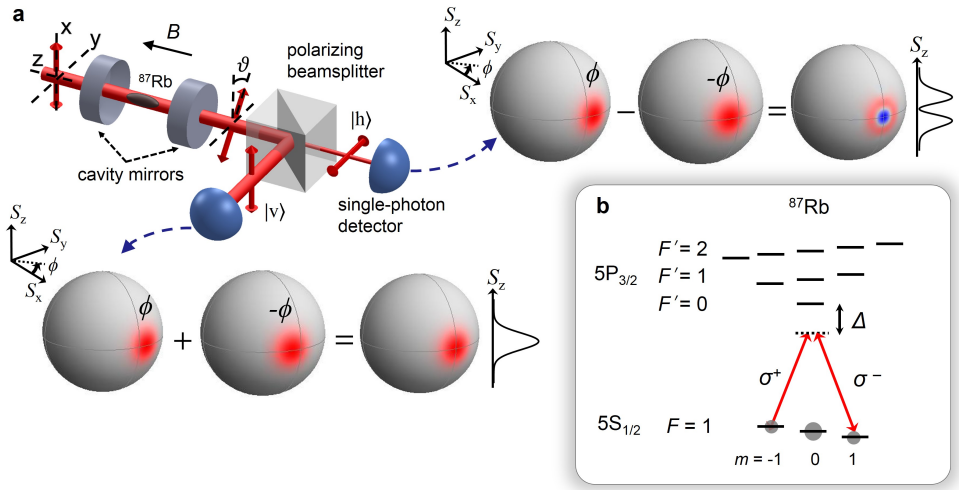

Figure 1. Scheme for heralded entanglement generation in a large atomic ensemble by single-photon detection. (a) Incident vertically polarized light experiences weak polarization rotation due to atomic quantum noise, and the detection of a horizontally polarized transmitted photon heralds an entangled state of collective atomic spin. An optical resonator enhances the polarization rotation and the heralding probability. The atoms are prepared in the product state of maximum S_x, the coherent spin state (CSS), before the heralding detection step. The atomic state is depicted on the Bloch sphere with a radius of $S = S_x$. (b) Atoms in the $5S_{1/2}, F = 1$ hyperfine manifold are coupled to the excited $5P_{3/2}$ manifold via linearly polarized light, decomposed into two circular polarization components $|\sigma^{\pm}\rangle$ that interact with the atomic ground-state *populations*. The outgoing polarization state of the light reflects the quantum fluctuations between the $|5S_{1/2}F = 1, m = \pm 1\rangle$ magnetic sublevels.

2. Photon polarization rotation by quantum spin noise

The pertinent atom-light interaction is enhanced by an optical cavity, into which we load $N_a = 3100 \pm 300$ laser-cooled ^{87}Rb atoms (Figure 1a). The atoms are prepared in the $5S_{1/2}, F = 1$ hyperfine manifold, such that each atom i can be associated with a spin $\vec{f}_i$, and the ensemble with a collective-spin vector $\vec{S} = \sum_i \vec{f}_i$. After polarizing the ensemble ($S_z \approx S$) by optical pumping, the collective spin state is rotated onto the $\hat{x}$ axis by means of a radiofrequency $\pi/2$ pulse, thus the atoms are prepared in the product state of maximum S_x. This (unentangled) initial state that is centered about $S_z = 0$ with a variance $(\Delta S_z)^2 = S/2$ is known as a coherent spin state (CSS). In our experiment, the atoms are non-uniformly coupled to the optical mode used for state preparation and detection, but the relevant concepts can be generalized to this situation [16].

Probe light resonant with a cavity mode, and red-detuned by $\Delta/(2\pi) = -200$ MHz from the ^{87}Rb transition $5^2S_{1/2}, F = 1$ to $5^2P_{3/2}, F' = 0$, is polarization analyzed upon transmission through the cavity. The vertical polarization state of each photon in the incident laser pulse $|\mathrm{v}\rangle = (|\sigma^+\rangle + |\sigma^-\rangle)/\sqrt{2}$ can be decomposed into two circular polarization components $|\sigma^{\pm}\rangle$

that produce opposite differential light shifts between the atomic magnetic sublevels $|m = \pm 1\rangle$. Hence a $|\sigma^{\pm}\rangle$ photon causes a precession of the collective spin vector $\vec{S}$ in the xy plane by a small angle $\pm\phi$ [17], and we denote the corresponding slightly displaced CSS by $|\pm\phi\rangle$. Then the combined state of the atom-light system after the passage of one photon can be written as

$$|\psi\rangle \propto |\sigma^{+}\rangle|+\phi\rangle + |\sigma^{-}\rangle|-\phi\rangle. \tag{1}$$

Conversely, atoms in the states $|m = \pm 1\rangle$ cause different phase shifts on the $\sigma^{\pm}$ photons, resulting in a net rotation of the photon linear polarization if the states $|m = \pm 1\rangle$ are not equally populated. Then the atomic quantum fluctuations between $|m = \pm 1\rangle$ in the CSS randomly rotate the polarization of the input photons $|\mathrm{v}\rangle$, giving rise to a nonzero probability $\propto \phi^2$ for an incident $|\mathrm{v}\rangle$ photon to emerge in the polarization $|\mathrm{h}\rangle = (|\sigma^{+}\rangle - |\sigma^{-}\rangle)/\sqrt{2}$, orthogonal to its input polarization. The detection of such a "heralding" photon projects the atomic state onto $\langle \mathrm{h}|\psi\rangle \propto |\phi\rangle - |-\phi\rangle$, which is not a CSS, but an entangled state of collective spin, namely, the first excited Dicke state [18] $|\psi_1\rangle$ along $\hat{x}$ (Figure 1a). In contrast, if the photon is detected in its original polarization $|\mathrm{v}\rangle$, the atomic state is projected onto $\langle \mathrm{v}|\psi\rangle \propto |\phi\rangle + |-\phi\rangle$, a state slightly spin squeezed [1]. This is because this photon detection outcome is most likely if the atomic spin S_z is near 0, so that the best estimate of the atomic state population distribution is now more tightly concentrated around $S_z = 0$ than it would be for the CSS. When $\phi \ll \sqrt{1/(2S)}$, the atomic state $\langle \mathrm{v}|\psi\rangle$ is essentially identical to the input CSS. The entangled atomic state $|\psi_1\rangle$ is post-selected by the detection of the heralding photon $|\mathrm{h}\rangle$.

In the experiment, the mean photon number in the incident laser pulse $k \sim 210$ is chosen such that the probability for one photon to emerge in heralding polarization $|\mathrm{h}\rangle$ is $p \approx 0.05 \ll 1$. This ensures a very small probability $\propto p^2$ for producing a different entangled state $|\psi_2\rangle$ heralded by two photons [17], a state which, due to our photon detection efficiency of $q = 0.3 < 1$, we would (mostly) mistake for $|\psi_1\rangle$. This admixture of $|\psi_2\rangle$ to the heralded state is suppressed by a factor of $3p(1-q) \approx 0.1$.

3. The effect of the optical dipole trap on the polarization rotation

The atoms are confined on the cavity axis by a far-detuned optical dipole trap at 852 nm with a linear polarization and the trap depth $U/h = 20(3)$ MHz. For our experiments, it is of utmost importance that the probe light polarization rotation ϑ be only caused by the desired effect, the collective atomic spin along the cavity axis, S_z, that exhibits quantum fluctuations around $\langle S_z\rangle = 0$. However, when the trap light polarization is not parallel or perpendicular to the probe, it can also change the probe polarization at 780 nm. Consider the simple case that the atoms are in the $F = 1$, $m = 0$ state. The trap light polarization is at angle $\varphi_{\mathrm{t}}/2$ with respect to the probe (Figure 2a). The probe field $|\sigma^{+}\rangle$, the trap field $|\sigma^{+}\rangle$ and $|\sigma^{-}e^{i\varphi_{\mathrm{t}}}\rangle$ can polarize the atoms through the third-order susceptibility and introduce a phase shift on the probe $|\sigma^{-}\rangle$ field, and vice versa. This is similar to the four-wave mixing process. The probe polarization rotation is proportional to $(U/\Delta)\phi \sin\varphi_{\mathrm{t}}$. This will obscure our desired polarization rotation signal coming from the atomic quantum spin noise in S_z. Only when the linear polarization of the trap light is aligned parallel or perpendicular to the probe light, this effect is diminished.

As a clean diagnostic, we prepare the atoms in the $F = 1$, $m = 0$ state, and measure the polarization rotation ϑ of the probe light as a function of the bias magnetic field B along the cavity axis, with the trap light briefly switched off or present during the measurement. Figure 2b shows that the trap light rotates the probe polarization in addition to the bias field B, resulting in an offset $\mu_B B/h = 3.1(2)$ MHz. Our calculation predicts the offset at $\mu_B B/h = 2.8(5)$ MHz when the trap polarization is at 45° to the probe. By aligning the trap linear polarization parallel to the probe polarization, the trap light no longer contributes to the rotation.

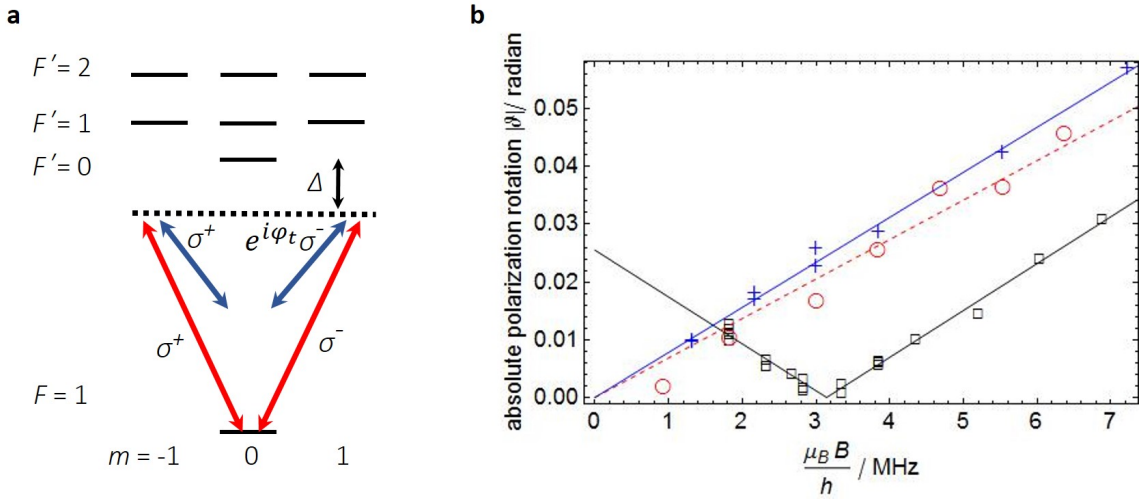

Figure 2. (Colour online) Probe light polarization rotation ϑ with the bias magnetic field B along the cavity axis for 4500 atoms in the $F = 1$, $m = 0$ state. (a) Atoms in the $F = 1$, $m = 0$ state are coupled to the excited states via the linearly polarized probe light (red arrows) and the linearly polarized trap light (blue arrows). The relative angle of the two linear polarizations is $\varphi_t/2$. (b) When the trap light is switched off the expected linear Faraday rotation is observed (red circles). The dashed red line is the prediction. When the trap light is present in the cavity and its linear polarization is not parallel or perpendicular to the probe light, it rotates the probe polarization in addition to the Faraday rotation, resulting in an offset (black squares). The solid black line is the fit. By aligning the trap polarization parallel to the probe, the effect of the trap light is diminished (blue crosses). The solid blue line is the fit.

4. Spin distributions and Wigner function

In order to reconstruct the collective-spin state generated by the heralding event, we rotate the atomic state after the heralding process by an angle $\beta = 0, \frac{\pi}{4}, \frac{\pi}{2}, \frac{3\pi}{4}$ about the $\hat{x}$ axis before measuring S_z. (Thus $\beta = 0$ corresponds to measuring S_z, $\beta = \pi/2$ corresponds to S_y, etc.) The measurement is performed by applying a stronger light pulse in the same polarization-optimized setup used for heralding. As the Faraday rotation angle $\vartheta \ll 1$ is proportional to S_z, and the probability for detecting $|\mathrm{h}\rangle$ photons is proportional to ϑ^2, the measured probability distribution of $|\mathrm{h}\rangle$ photon number, $g(n_\beta)$, reflects the probability distribution of S_β^2. Figure 3a shows that a single heralding photon substantially changes the spin distribution towards larger values of $\langle S_\beta^2 \rangle$. Here we show the measurement for $\beta = 0$ only. For other rotation values β see [16]. We further verify that the heralded state remains (nearly) spin polarized with a contrast of $\mathcal{C} = 0.99^{+0.01}_{-0.02}$, the same as for the CSS within error bars.

From the photon distributions $g(n_\beta)$ we can reconstruct the density matrix ρ_{mn} in the Dicke state basis [18] along $\hat{x}$, where $|n = 0\rangle$ denotes the CSS along $\hat{x}$, $|n = 1\rangle$ the first Dicke state, $|n = 2\rangle$ the second Dicke state, etc. From the density matrix we obtain the Wigner function $W(\theta, \phi)$ on the Bloch sphere [19] (Figure 3e). To accurately determine the Wigner function value on the axis, $W(\theta = \frac{\pi}{2}, \phi = 0) = \sum_n (-1)^n \rho_{nn}$, that depends only on the population terms ρ_{nn}, we average the photon distributions $g(n_\beta)$ over four angles β and thereby reduce the fitting parameters to just $\rho_{nn}, n \leq 4$. This is equivalent to constructing a rotationally symmetric Wigner function from the angle-averaged marginal distribution [20]. We obtain $\rho_{00} = 0.32 \pm 0.03, \rho_{11} = 0.66 \pm 0.04$ with negligible higher-order population terms, giving $W(\frac{\pi}{2}, 0) = -0.36 \pm 0.08$, to be compared to $W(\frac{\pi}{2}, 0) = -1$ for the perfect first Dicke state.

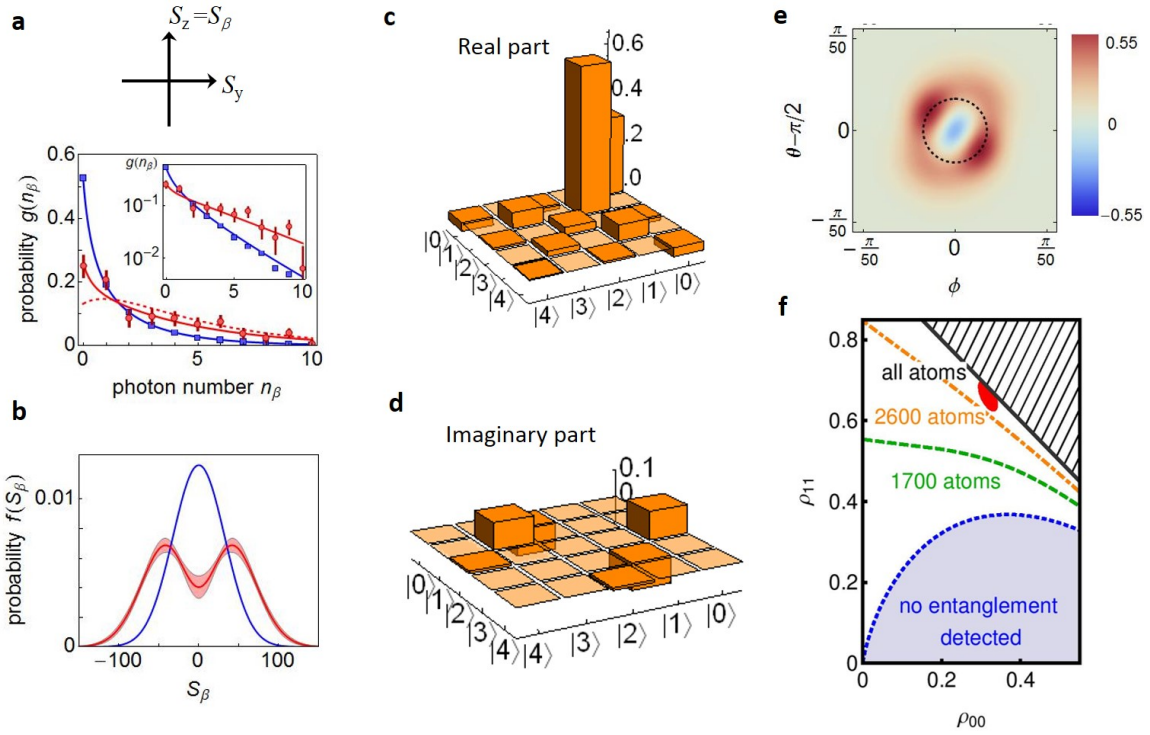

Figure 3. (Colour online) (a) Measured photon distributions $g(n_\beta)$ for no heralding photon detected (blue squares), and for one heralding photon detected (red circles) for rotation angles $\beta = 0$, i.e., $S_\beta = S_z$. For other rotation values β see [16]. Inset: Logarithmic representations of the same data. The solid blue and the dashed red curves are predictions without any free parameters, for the CSS and the perfect first Dicke state, respectively. The solid red line is the fit. (b) Reconstructed collective spin distributions of the heralded state (red) for $\beta = 0$. The spin distributions of the CSS (blue) are for reference. (c),(d) Real and imaginary parts of the reconstructed density matrix elements, in the Dicke state basis along $\hat{x}$, for the heralded state. (e) Reconstructed Wigner function $W(\theta, \phi)$ for the heralded state on the Bloch sphere [19]. θ is the polar angle with respect to $\hat{z}$ and ϕ is the azimuthal angle with respect to $\hat{x}$. The first excited Dicke state and the CSS have $W(\frac{\pi}{2}, 0) = -1$ and $W(\frac{\pi}{2}, 0) = 1$, respectively. To provide a reference scale for the size of the negative region, the black dashed line is the contour at which the CSS has a Wigner function value $1/e$. (f) Entanglement depth criterion [13] for the heralded state, plotted in terms of density matrix elements ρ_{00} and ρ_{11}. The red shaded region represents the 1 s.d. confidence region for the heralded state. Lines represent boundaries for k-particle entanglement in terms of atom number N_a; a state with ρ_{11} greater than such a boundary displays at least k-particle entanglement.

We can also fit the density matrix including the coherence terms simultaneously to $g(n_\beta)$ for all four angles β, without angle-averaging. Since the photon distributions $g(n_\beta)$ measure the distributions of S_β^2, they cannot contain any odd power of S_β. In general, for a given spin distribution $f(S_\beta)$, the distribution function of S_β^2, $G(S_\beta^2) = \frac{1}{2|S_\beta|}\Big(f(S_\beta) + f(-S_\beta)\Big)$. The distribution $f(S_\beta)$ contains even functions of S_β for ρ_{mn} where $m+n$ is even, and odd functions of S_β for ρ_{mn} where $m+n$ is odd, therefore the distribution $G(S_\beta^2)$ and hence the photon number distribution $g(n_\beta)$ contain the contribution of only the even terms of the density matrix ρ_{mn}, and have no information of odd ρ_{mn} terms.

In order to display the Wigner function, we bound the odd ρ_{mn} terms by verifying that the heralding process does not displace the state relative to the CSS. This is accomplished by performing a measurement with an auxiliary probe beam polarized at 45 degrees relative to $|\mathrm{v}\rangle$, such that the difference between the measured $|\mathrm{h}\rangle$ and $|\mathrm{v}\rangle$ photon numbers is proportional to S_z. We find a heralding-light-induced shift $\delta\langle S_z\rangle = -0.2 \pm 1.6$, consistent with zero, and very small compared to the CSS rms width $(\Delta S_z)_{\mathrm{CSS}} \approx 30$. Therefore we set the odd terms to zero, and display the resulting density matrix and corresponding Wigner function in Figure 3c-e. The spin distributions $f(S_z)$ obtained from this density matrix are shown in Figure 3b.

If we calculate $W(\frac{\pi}{2}, 0)$ from the density matrix without angle-averaging, we find $W(\frac{\pi}{2}, 0) = -0.27 \pm 0.08$, within error bars consistent with the angle-averaged value. Note that $W(\frac{\pi}{2}, 0)$ only depends on even ρ_{mn} terms, therefore can be fully determined by the measured photon distributions $g(n_\beta)$.

In order to quantify the minimum number of mutually entangled atoms, we use a criterion derived in Ref. [13] that establishes entanglement depth as a function of the populations ρ_{00} and ρ_{11}. From this criterion, generalized to the case of non-uniform coupling to the measurement light field, we deduce an average entanglement depth of $\mathcal{N}_a = 2910 \pm 190$ out of $N_a = 3100$ atoms (Figure. 3f) using the angle-averaged density matrix. Our results represent the first experimental verification of the mutual entanglement shared by virtually all atoms in an ensemble that contains more than a few particles.

5. Discussion and conclusion

In our system, the maximum atom number of ~ 3000 is set by the accuracy of the spin rotation, and can be increased by two orders of magnitude by better magnetic-field control [10]. The achieved state fidelity $\rho_{11} = 0.66 \pm 0.04$ is below the value of $\rho_{11} = 0.73$ required for the Fisher information [14] to exceed that of the CSS. It is limited by a number of factors. At our atom number N_a and the polarization rotation strength ϕ, the polarization impurity $\sim 3 \times 10^{-5}$ of the entire setup gives rise to false heralding events equal to 10% of the quantum spin signal from the CSS. This impurity is also present in the measurement process. In addition, the atoms confined in the optical trap at finite temperature have temporal fluctuations in their coupling strength to the heralding laser pulse and the measurement laser pulse, resulting in $\sim 5\%$ admixture of the CSS to the measured heralded state. The fidelity is further reduced by phase broadening of the atomic state by the heralding laser pulse and by magnetic field fluctuations. Increasing the atom-cavity interaction strength can reduce the false detection events and the atomic state phase broadening. Combined with improved stabilization of the magnetic field, these changes can increase the fidelity and enable more highly-entangled states to be produced.

The above results demonstrate that even with limited resources, i.e. weak atom-photon coupling, heralding schemes can be used to boost the effective interaction strength by a large factor, enabling the production of highly entangled states [21, 17]. Furthermore, by repeated trials and feedback the entanglement generation can be made quasi-deterministic [22, 23]. Our approach is related to other heralded schemes for quantum communication [22, 24, 23, 25] and entangled-state preparation [26, 27, 28], and it would be interesting to generalize the present analysis to infer characteristics of the atomic state from the measured optical signals in those experiments. We note that the same first Dicke state was created in an ensemble of up to 41 atoms with a scheme that uses many heralding photons in a strongly coupled atom-cavity system [13]. The detection of two or more photons prepares Schrödinger cat states [17] of the atomic ensemble with more metrological gain. We expect that heralded methods can generate a variety of nearly pure, complex, strongly entangled states that are not accessible by any other means at the present state of quantum technology.

References

[1] Kitagawa M and Ueda M 1993 *Phys. Rev. A* **47** 5138–5143
[2] Appel J, Windpassinger P J, Oblak D, Hoff U B, Kjærgaard N and Polzik E S 2009 *Proceedings of the National Academy of Sciences* **106** 10960–10965
[3] Takano T, Tanaka S I R, Namiki R and Takahashi Y 2010 *Phys. Rev. Lett.* **104** 013602
[4] Schleier-Smith M H, Leroux I D and Vuletić V 2010 *Phys. Rev. Lett.* **104** 073604
[5] Leroux I D, Schleier-Smith M H and Vuletić V 2010 *Phys. Rev. Lett.* **104**(7) 073602
[6] Gross C, Zibold T, Nicklas E, Estève J and Oberthaler M K 2010 *Nature* **464** 1165–1169
[7] Riedel M F, Böhi P, Li Y, Hänsch T W, Sinatra A and Treutlein P 2010 *Nature* **464** 1170–1173
[8] Hamley C D, Gerving C G, Hoang T M, Bookjans E M and Chapman M S 2012 *Nat Phys* **8** 305 – 308
[9] Sewell R J, Koschorreck M, Napolitano M, Dubost B, Behbood N and Mitchell M W 2012 *Phys. Rev. Lett.* **109** 253605
[10] Bohnet J G, Cox K C, Norcia M A, Weiner J M, Chen Z and Thompson J K 2014 *Nat Photon* **8** 731–736
[11] Leibfried D, Knill E, Seidelin S, Blakestad R B, Chiaverini J, Hume D B, Itano W B, Jost J D, Langer C, Ozeri R, Reichle R and Wineland D J 2006 *Nature* **438** 639–642
[12] Monz T, Schindler P, Barreiro J T, Chwalla M, Nigg D, Coish W A, Harlander M, Hänsel W, Hennrich M and Blatt R 2011 *Phys. Rev. Lett.* **106** 130506
[13] Haas F, Volz J, Gehr R, Reichel J and Estéve J 2014 *Science* **344** 180–183
[14] Strobel H, Muessel W, Linnemann D, Zibold T, Hume D B, Pezz L, Smerzi A and Oberthaler M K 2014 *Science* **345** 424–427
[15] Lücke B, Peise J, Vitagliano G, Arlt J, Santos L, Tóth G and Klempt C 2014 *Phys. Rev. Lett.* **112**(15) 155304
[16] McConnell R, Zhang H, Hu J, Ćuk S and Vuletić V 2015 *Nature* **519** 439–442
[17] McConnell R, Zhang H, Ćuk S, Hu J, Schleier-Smith M H and Vuletić V 2013 *Phys. Rev. A* **88**(6) 063802
[18] Arecchi F T, Courtens E, Gilmore R and Thomas H 1972 *Phys. Rev. A* **6**(6) 2211–2237
[19] Dowling J P, Agarwal G S and Schleich W P 1994 *Phys. Rev. A* **49**(5) 4101–4109
[20] Lvovsky A I, Hansen H, Aichele T, Benson O, Mlynek J and Schiller S 2001 *Phys. Rev. Lett.* **87** 050402
[21] Agarwal G S, Lougovski P and Walther H 2005 *Journal of Modern Optics* **52** 1397–1404
[22] Duan L M, Lukin M D, Cirac J I and Zoller P 2001 *Nature* **414** 413–418
[23] Matsukevich D N, Chaneliere T, Jenkins S D, Lan S Y, Kennedy T A B and Kuzmich A 2006 *Phys. Rev. Lett.* **97** 013601
[24] Kuzmich A, Bowen W P, Boozer A D, Boca A, Chou C W, Duan L M and Kimble H J 2003 *Nature* **423** 731–734
[25] Simon J, Tanji H, Thompson J K and Vuletić V 2007 *Phys. Rev. Lett.* **98** 183601
[26] Choi K S, Goban A, Papp S B, van Enk S J and Kimble H J 2010 *Nature* **468** 412 – 416
[27] Christensen S L, Beguin J B, Sorensen H L, Bookjans E, Oblak D, Müller J H, Appel J and Polzik E S 2013 *New Journal of Physics* **15** 015002
[28] Christensen S L, Béguin J B, Bookjans E, Sørensen H L, Müller J H, Appel J and Polzik E S 2014 *Phys. Rev. A* **89**(3) 033801